

The Effect of Oxygen Concentration on the Structure of Turbulent Nonpremixed Flames

B.B. Dally¹, A. N. Karpetis² and R.S. Barlow²

¹Department of Mechanical Engineering
Adelaide University, South Australia, 5005 AUSTRALIA

²Combustion Research Facility
Sandia National Laboratories, Livermore, CA, USA

Abstract

MILD combustion is a newly implemented and developed concept to achieve high thermal efficiency and fuel saving while maintaining emission of pollutants at very low levels. It utilizes the concept of heat and exhaust gas recirculation to achieve combustion at reduced temperature, with a flat thermal field and low turbulence fluctuations. An experimental burner is used in this study. Temporally, and spatially resolved measurements of reactive scalars are conducted on three different flames of H₂/CH₄ fuel mixture at fixed jet Reynolds number and different oxygen mass fractions in the hot oxidant stream. The results show substantial variation of the flame structure with the decrease of the oxygen level. The results also point towards a different chemical pathway for the reaction in this combustion regime, where the formation of the OH radical and NO is less dependent on temperature.

Introduction

Abatement of pollutants emitted from combustion systems is still a relevant topic of research despite the attention it was given during the last decade. Many of the techniques developed to reduce pollutants emission, such as NO_x, SO_x and CO, did not satisfy the regulatory constraints or resulted in a financial penalty due to reduced thermal efficiency and productivity.

MILD (Moderate and Intense Low Oxygen Dilution) Combustion, also known as Flameless Oxidation (FLOX[®]), is a newly developed and implemented technique to achieve very low emission of pollutants and improve thermal efficiency of combustion systems[6][7][10]. MILD Combustion takes place at reduced temperature in the range of 1100-1500K, and it is characterized by a flat thermal field, minor temperature fluctuations, and, at optimised conditions, no visible or audible flame, hence the name (Flameless). Although the concepts utilized in the MILD Combustion have been known for quite sometime, valuable knowledge on the structure of these flames under MILD Combustion is yet to be explored.

Katsuki and Hasegawa [7] published a review paper on MILD combustion. They found that intense mixing of the combustion air with burnt gases in the furnace, produced by high momentum ejection of combustion air, lowers the flame temperature and yields distributed reactions. They also found that in addition to highly preheated air, intense mixing of the air with plenty of burnt gases before combustion is essential to achieve low NO_x emission. They concluded that (i) there is an excellent potential for this technology to narrow the gap between the two objectives of low pollutants emission and fuel savings and (ii) the application of this combustion regime to other potential industrial systems requires better understanding of the change of flame structure at low oxygen levels and the effect of the turbulence on this structure.

Weber et al.[9] found that in comparison to conventional furnace systems, MILD combustion has the capacity to increase the net radiation flux by up to 60%.

This paper is part of a concerted effort to look at the structure of flames under gas and heat recirculation conditions including the MILD Combustion regime. Experimental and computational efforts are underway to look at issues such as chemistry pathway, interaction between turbulence and chemistry, effects of mixing, and the applicability of current combustion models to predict this combustion regime. In this paper the effects of oxygen concentration in the hot oxidant stream on the structure of turbulent non-premixed flames are presented.

Experimental Setup JHC Burner Assembly

A laboratory scale experimental burner was used in this study. This burner is referred to as Jet in Hot Coflow (JHC). Figure 1 shows a cross section of the JHC burner design. It consists of an insulated and cooled central jet (ID=4.25mm) and an annulus (ID=82mm) with a secondary burner mounted upstream of the exit plane. The secondary burner provides hot combustion products, which are mixed with air and nitrogen via two side

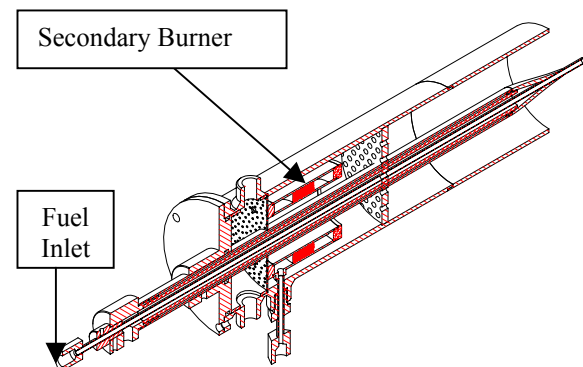


Figure 1 Cross-section of Jet in Hot Coflow Burner

inlets at the bottom of the annulus to control the O₂ levels in the mixture. The cold mixture of air and nitrogen also assists in cooling the secondary burner. The burner can operate at a wide range of coflow temperatures and O₂ levels. The burner allows easy optical access to measure boundary conditions at the exit plane. The outer annulus is insulated using ceramic straps to minimize heat loss to the surroundings. The coflow stream is wide enough to sustain the same conditions close to the reaction zone for the full length of laminar flames. For turbulent flames some mixing with fresh air from the surroundings starts to have an effect at ~100 mm above the jet exit plane.

Experimental Facility

Experiments were conducted at the Combustion Research Facility at Sandia National Laboratories, Livermore California. The single-point Raman-Rayleigh-LIF technique was used in this

study. This technique is well developed, providing simultaneous, quantitative, spatially and temporally resolved measurement [5] of temperature, concentration of major species CH_4 , H_2 , H_2O , CO_2 , N_2 and O_2 and minor species, NO , CO and OH . Figure 2 shows a schematic of the laser diagnostics setup at Sandia. This setup was described in numerous publications [2, 4, and 5] and will not be described in this paper due to lack of space.

A mixture of H_2 and CH_4 , equal in volume, was used as the fuel in the central jet. The same fuel mixture was also used in the secondary burner and the products were mixed with N_2 and air to control the oxygen concentration and temperature in the annulus. The temperature of the mixture in the annulus was fixed at $\sim 1300\text{K}$ for all experiments. For low jet Reynolds number flames the fuel mixture in the jet was heated slightly, despite the insulation and cooling of the central jet. Table 1 shows the different operating conditions of the cases studied.

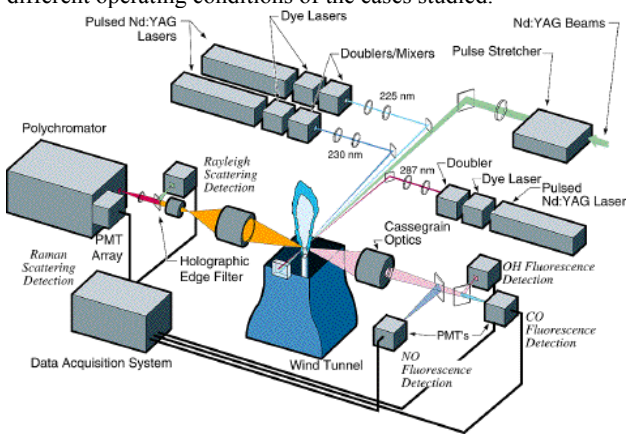


Figure 2 Single-Point Raman-Rayleigh-LIF Setup at Sandia National Laboratory

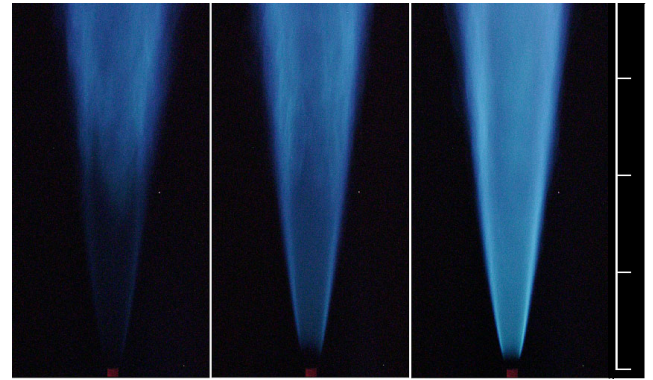
Table 1: Operating Conditions for Cases Studied

Fuel Jet (CH_4/H_2)			Oxidant Coflow				
Case	Re#	T(K)	T(K)	YO_2 %	YN_2 %	YH_2O %	YCO_2 %
HM1	9482	305	1300	3	85	6.5	5.5
HM2	9482	305	1300	6	82	6.5	5.5
HM3	9482	305	1300	9	79	6.5	5.5

Results and Discussion

Figure 3 shows photographs of the three flames listed in Table 1 taken at the same exposure time. It is clear that, when the oxygen mass fraction in the oxidant stream is reduced, the flame luminosity is reduced due to the suppression of certain radicals in the flame. These radicals, which are apparent at high temperature flames, seem to have lower concentration in these flames. This only adds to the evidence that this type of flame has a different chemical path than ordinary flames. Entertainment from the surrounding air starts to have an effect on the flame at $\sim 100\text{mm}$ above the jet. This can be seen in the photographs where the flame luminosity increases at the top part of the flame.

Figure 4 shows radial profiles of mean temperature and mass fractions of OH , CO and H_2O for flames HM1, HM2 and HM3 at an axial location 30mm above the jet exit. The temperature plot shows a dropped in peak mean temperature from 1700K in HM3 to 1400K in HM1, and this is due to the decrease of oxygen mass fraction in the hot oxidant stream. The temperature at the centerline is $\sim 420\text{K}$ and is the same for all cases. The temperature distribution in annulus side is also consistent between all flames and we can safely assume that a relatively uniform temperature is maintained in the oxidant stream.



HM1 HM2 HM3

Figure 3 Photographs of flames HM1, HM2 and HM3

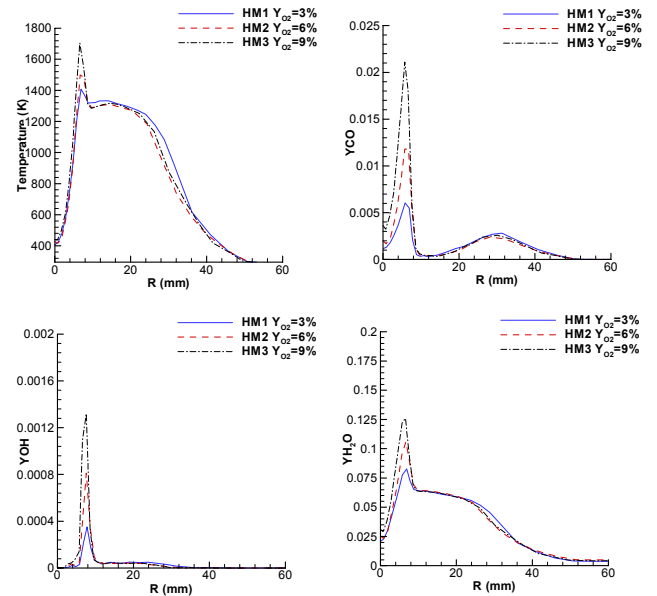


Figure 4 Radial Profiles of Temperature and mass fractions of OH , O_2 and H_2O at axial location $Z=30\text{mm}$ for flames HM1 (solid), HM2 (dashed) and HM3 (dash-dotted)

The OH plot shows a 3.5 fold decrease in the mass fraction of OH , when the oxygen level is decreased from 9% to 3%. Also noticeable is that reaction zone is almost 4mm in width for all flames. A slight shift of peak OH towards the oxidant side can be seen in the HM1 case as compared to the HM3 case.

The CO plot is consistent with that of OH and temperature, in that the CO drops by four folds in flame HM1 when compared to the level in flame HM3. The drop can also be seen at the centerline although the temperature at this location is similar for all cases. This is understandable since all the CO in the centerline is due to diffusion from the reaction zone. The CO ‘‘hump’’, which appears in the oxidant stream, is the same for all cases and must have been caused by the cooling of the flame by the outer burner wall. Very low level of CO at radial locations 10mm to 16mm can be seen which implies that the effect of the CO in the oxidant stream on the reaction zone is negligible.

The H_2O plot shows the same trend as those discussed before. The H_2O drops from 12.5% in flame HM3 to 8% in flame HM1. Similar distribution is found in the oxidant stream for all cases.

Figure 5 shows radial profiles of temperature and mass fractions of OH , CO and H_2O for flames HM1, HM2 and HM3 at an axial

location 120mm above the jet exit. At this location air from the tunnel mixes with the hot oxidant stream and the initial oxygen level is no longer maintained. Nonetheless the temperature peak is very similar to that observed earlier at an axial location of 30mm above the jet. The major difference in the temperature distribution is in the centerline value with a 200K difference between HM1 and HM3 flames.

The OH plot shows similar ratios between the peak levels for the different flames, with the peak values dropping by half when compared to peaks at axial location 30mm above the jet exit. This indicates that composition may have affected the production of OH and not the temperature. This plot also shows that the width of the reaction zone is smaller for the HM1 flame when compared to the HM3 flame. The temperature distribution at this location is also consistent with this observation.

The CO plot shows a ~30% increase in peak levels when compared to the peak levels at axial location of 30mm. The overall peak level ratios between the different flame remains the same.

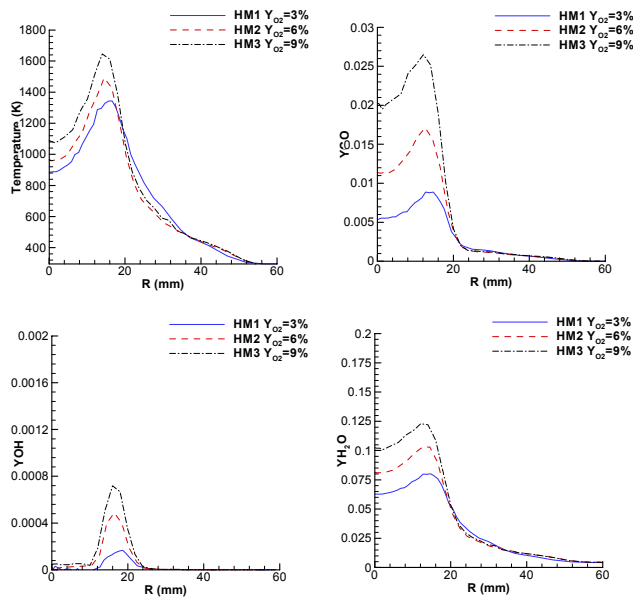


Figure 5 Same as Figure 4 except that this data is at axial location 120mm

Noticeable, however, is the large increase of CO mass fraction in the centerline for all cases. This may have some implication on the amount of CO produced in the reaction zone of these flames when compared to standard diffusion flames but it is likely to be a matter of the downstream decay of the centreline value of mixture fraction. The previous “hump” in CO distribution, originating in the oxidant stream, has been consumed at this axial location.

The H_2O profiles are similar to those seen earlier except that the centerline values have increased to ~80% of the peak flame level.

Figure 6 shows radial profiles of oxygen mass fraction for flames HM1, HM2 and HM3 plotted at four axial locations, 4mm, 30mm, 60mm and 120mm. This figure shows that the tunnel air for locations below 120mm does not affect the oxygen mass fraction at the vicinity of the jet. At axial location 120mm above the jet the oxygen distribution is consistent for all cases albeit the wider distribution for the flame HM1.

Figure 7 shows radial profiles of mean NO mole fractions for the same flames and locations as in Fig. 6. The NO distribution for flame HM1 is totally different from the other two flames. At the first axial location (4mm) the NO distribution is quite wide and is almost three times that of other flames. At this location some small lift off was observed as can be seen in the photographs (Fig. 3) and that may be the reason for the difference in peak NO. The NO mole fractions for flame HM1 at locations 30mm, 60mm

and 120mm have the same peak of 2.5 ppm. For flames HM2 and HM3 the NO distribution is inconsistent with that of flame HM1. A distinct peak close to the reaction zone location appears for both flames. At location 30mm and 120mm flame HM2 has NO peak level which is almost half that of the peak level for flame HM3 while at location 60mm the peak level for both flames is similar. Worth noting that the peak temperature is roughly the same for all locations and that NO level is very small when compared with standard diffusion flames with similar Reynolds number. This indicates that chemical effects are present and that different NO mechanisms may be active at different parts of the flame.

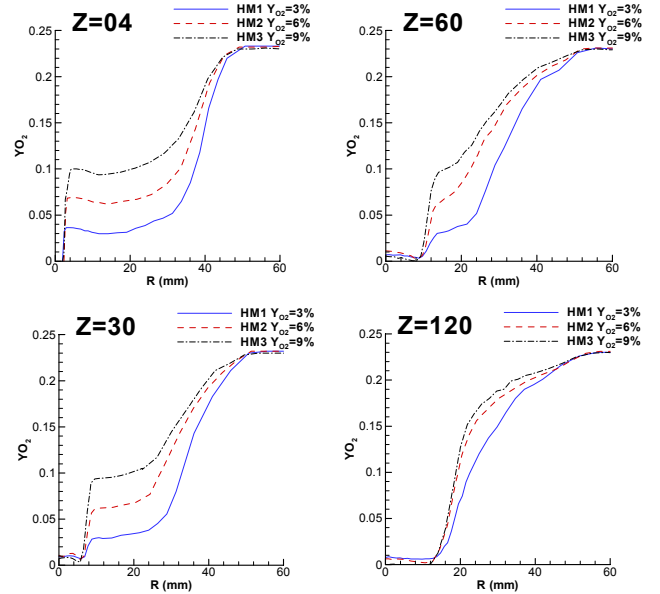


Figure 6 Radial profiles of oxygen mass fraction at different axial locations and for flames HM1 (solid), HM2 (dashed) and HM3 (dash-dotted)

The results presented above are quite unique in their scope and in the trends they presented. The carefully planned experiments have isolated the effects of turbulent intensity, products concentration and temperature in order to solely investigate the effect of oxygen concentration.

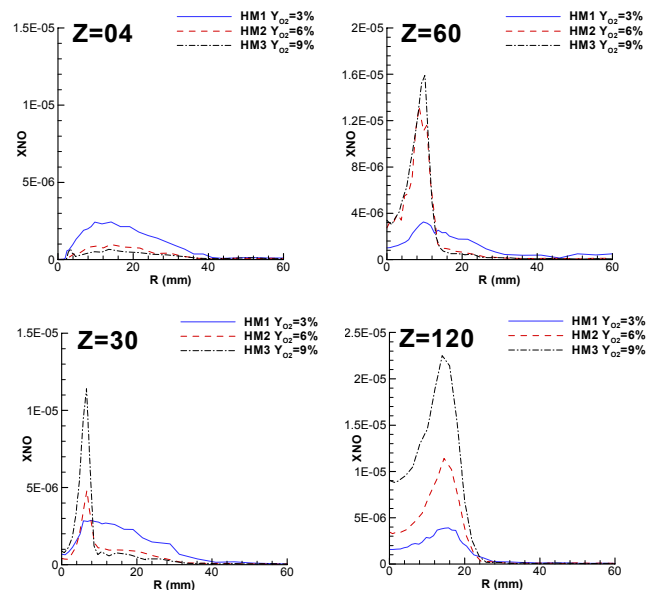


Figure 7 Radial profiles of NO mole fractions at different axial locations and for flames HM1 (solid), HM2 (dashed) and HM3 (dash-dotted)

It is found that changing the oxygen concentration leads to substantial changes to flame structure and NO emission. It is also found that at 3% oxygen a different chemical mechanism controls the production and consumption of NO and the dependence on temperature is much less apparent.

It is thus believed that a better understanding on the chemical pathway at reduced temperatures is required in order to better understand these trends and examine the applicability of existing mechanisms to these flames.

Previous computational study by Dally [3] has found that existing high temperature chemical kinetics mechanisms cannot be applied to these flames and low temperature chemical kinetics mechanism need to be used instead. Similar trends to those found here were also identified in these calculations and in particular the importance of the CH₂OH species as a low temperature species was identified. Future work will aim at simultaneously measure OH, CH₂OH and temperature in order to monitor the relation between their concentration level and the oxygen concentration and that of the temperature.

The data collected in this study will be available on the web site in the near future as part of the International Workshop on Measurements and Computation of Turbulent Nonpremixed Flame (TNF) [1].

Conclusions

Detailed measurement of temperature, major and minor species were presented in this paper. The measurements were conducted on three flames of methane and hydrogen mixture stabilised on the JHC burner at three different oxygen concentrations in the oxidant stream. The coflow contained hot products at 1300K in the immediate vicinity of the jet and the burner was mounted on a wind tunnel running air at atmospheric conditions. The Reynolds number was kept constant for all flames. The data showed that reducing the oxygen mass fraction from 9% to 3% in the hot oxidant stream results in substantial changes to the flame structure. These changes include peak temperature drop of up to 400K, three-fold drop in OH and CO levels and a different radial distribution of temperature for the HM3 case. The data points towards a different mechanism and chemical pathway for these flames when compared with standard atmospheric flames, especially for the OH and NO formation. The trends for quantities measured in consistent with previous results obtained computationally for laminar flame data.

Acknowledgments

Dr. Dally acknowledges the support of the Australian Research Council. Dr. Dally also thanks the CRF at Sandia for their generous support during his visit and for making their facilities available to conduct the experiments. Drs. Karpets and Barlow are supported by the United States Department of Energy, Office of Basic Energy Sciences, Division of Chemical Sciences.

References

- [1] Barlow, R.S., Combustion Research Facility, Sandia National Laboratory, <http://www.ca.sandia.gov/tdf/Workshop.html>
- [2] Dally, B.B., Masri, A.R. Barlow, R.S, and Fiechtner, G.J., *Combust. Flame*, vol 114/1-2, pp.119-148, 1998
- [3] Dally, B.B., *The 1999 Australian Symposium on Combustion*, Newcastle, 1999
- [4] Dally, B.B., Masri, A.R. and Fletcher, D.F., *Combust. Theory and Modelling*, 2 (1998) 193-219
- [5] Dally, B.B., Masri, A.R. Barlow, R.S, Fiechtner, G.J. and Fletcher, D.F., *Twenty-Sixth Symposium (International) on Combustion*, Combustion Institute, Pittsburgh, PA, 1996, vol 2, pp. 2191-2197.
- [6] Plessing, T. Peters, N. and Wüning, J.G., *Twenty-Seventh Symposium (International) on Combustion*, Combustion Institute, Pittsburgh, PA, 1998, vol. 2, pp. 3197-3204.
- [7] Katsuki, M. and Hasegawa, T., *Twenty-Seventh Symposium (International) on Combustion*, Combustion Institute, Pittsburgh, PA, 1998, vol. 2, pp. 3135-3146
- [8] Masri, A.R., Barlow, R.S. and Dibble, R., *Prog. Energy Combust. Sci.*, vol. 22, 307-362, 1996
- [9] Weber, R, Verlaan Ad L., Orsino S. and Lallemand, N., *Journal of the Institute of Energy*, September 1999, 72, pp. 77-83
- [10] Wüning, J.A. and Wüning, J.G., *Progress in Energy and Combustion Science*, Vol. 23, pp. 81-94, 1997